Flow Control and Passive Low Noise Technologies for Landing Gear Noise Reduction

Bennett, Gareth J.; Lai, Jiang; O'Brien, Gordon C.; Ragni, D.; Avallone, F.; Rubio Carpio, A.; Pott-Pollenske, Michael

DOI
10.2514/6.2022-2848

Publication date
2022

Document Version
Final published version

Published in
28th AIAA/CEAS Aeroacoustics 2022 Conference

Aeroacoustics Conferences
June 14-17, 2022, Southampton, UK
28th AIAA/CEAS Aeroacoustics 2022 Conference

10.2514/6.2022-2848

Flow Control and Passive Low Noise Technologies for Landing Gear Noise Reduction

Gareth J. Bennett*, Jiang Lai† and Gordon O'Brien‡
Trinity College Dublin, the University of Dublin, D02 PN40, Ireland

Daniele Ragni§, Francesco Avallone¶, Alejandro Rubio Carpio‖
Delft University of Technology, Kluyverweg 1, 2629HS, Delft, The Netherlands.

Michael Pott-Pollenske **
DLR, German Aerospace Center, 38108 Braunschweig, Germany

This paper examines the use of both flow control and passive low noise technologies to reduce the aerodynamic noise radiated from a modified LAGOON landing gear, as tested in the EU funded H2020 collaborative research project: INVENTOR, InnoVative dEsign of iNstalled airframe componenTs for aircraft nOise Reduction. At approach to landing, landing gear noise is still a significant contributor to environmental noise in the vicinity of airports. Progress is being made with ambitious projects which aim to develop significantly reconfigured aircraft architectures to reduce airframe noise. The current project examines noise abatement measures which could be retrofit to existing landing gear configurations. Flow control in the form of low TRL "air curtains" which form a fluidic shield or virtual fairing are examined. Amongst the most interesting passive solutions are a selection of higher TRL porous materials in the form of wire mesh, perforated plates and 3D materials. In order to provide a simplified baseline landing gear mock-up on which to test the low noise technologies, the LAGOON NLG is modified with the addition of a torque-link and brakes and is called the "LAGOON-SLG". The porous materials are assessed experimentally in the A-Tunnel aeroacoustic facility in TU Delft, the Netherlands and the air curtains are examined in DLRs AWB aeroacoustic facility in Braunschweig, Germany.

I. Nomenclature

LNT	=	Low Noise Technology
FDM	=	Fused Deposition Modelling
$MSLA$	=	Masked Stereolithography
Lac	=	Local Air Curtain
$MVAC$	=	Multiple Velocity Air Curtain

II. Introduction

Landing gear is mechanically complex, primarily designed to support the load of a landing aircraft. Its design, as a priority, is constrained by requirements associated with safety, inspection and maintenance. This has resulted in a large number of components clustered together in a highly non-aerodynamic shape. Whilst it should be an easy task to dramatically decrease landing gear noise by fully encasing it in a solid aerodynamic fairing, the overriding requirements of weight and safety prevent this obvious solution from being adopted. Therefore, unlike the aeroengine which has been

*Associate Professor, School of Engineering, Parsons Building, gareth.bennett@tcd.ie, Senior AIAA Member.
†Graduate Student, School of Engineering, Parsons Building.
‡Chief Technical Officer, Specialist, School of Engineering, Parsons Building.
§Associate Professor, Department of Flow Physics and Technology
¶Assistant Professor, Department of Flow Physics and Technology
‖Reseach Fellow, Department of Flow Physics and Technology
**Research Scientist. Institute of Aerodynamics and Flow Technology, Lilienthalplatz 7

acoustically refined over 50 years, current production aircraft landing gear are almost completely absent of any design or noise abatement technology which might lower its significant acoustic output.

A. Air Curtain Technology and Permeable Flow Fairings

Several noise reduction technologies are based upon preventing aerodynamic flow interaction with the landing gear that creates sources of noise either at the surface or in the region downstream the model. One of these technologies is the use of an "air curtain", which is really a planar jet in cross-flow, as a noise reduction technology for aircraft landing gear. Air curtains have previously been used in a wide variety of engineering applications from wind tunnel blockage [1], smoke and heat transfer shields [2, 3] as well as for the creation of barriers to prevent the escape of infectious airborne particles from biological safety cabinets [4]. To the authors knowledge, it was first suggested as a technology for landing gear noise reduction in a patent by Wickerhoff and Sijpkes [5] although no further development of this paper-based proposal by the inventors themselves is evident. However, a European Union funded project: TIMPAN, did investigate a simplified geometry of the concept experimentally and measured noise reductions of between 3dB and 10dB and concluded that for full models larger noise reductions could be anticipated [6]. The TIMPAN research demonstrated a proof-of-concept to significantly reduce broadband landing gear noise which typically scales with the 6^{th} power of local flow speed. The authors of the TIMPAN work also identified potential obstacles to the adoption of this technology, *viz.* the noise generated from the introduction of the air curtain itself. They found that this additional noise was composed of two separate noise sources: a high frequency jet-mixing noise that scales with the 8^{th} power of the planar jet velocity and a lower frequency lip-noise source found at the planar jet exit slot which scales with the 5^{th} power.

Figure 1 illustrates the concept of how an air curtain in cross-flow might reduce the aerodynamic noise from landing gear on approach to landing. Three possible configurations are shown. The first, figure 1(a), shows how the air curtain issues from the fuselage upstream of the landing gear at some fixed angle relative to the aircraft velocity vector. The air curtain streamlines would subsequently follow a curvature primarily dependent on the angle of emission and the velocity ratio between the planar jet velocity and the local mean velocity over the fuselage. Figure 1(b) shows an alternative configuration where air curtains issue from a vertical strut located upstream of the landing gear and this two-sided lateral blowing set-up is described as being similar to a large streamline cap [6]. The third alternative, shown in Fig. 1(c), would route the air supply along the landing gear itself to provide local jets for local shielding.

Each of these implementations have advantages and disadvantages. Fig. 1(a) would issue from the fuselage and could provide complete shielding of the landing gear. This could be turned off just upon landing and thus allow essential airflow for brake cooling and not impede visual safety inspection by ground staff. However, it would require the most mass flow supply of air and the high jet velocity required to shield the entire length of leg might result in a significant additional noise source. Fig. 1(b), would require a much lower exit velocity being required to only extend to half the width of the gear, at most, but would require a retractable strut to extend from the fuselage. The third implementation, in Fig. 1(c), would have the lowest required mass flow, lowest additional noise but would add some complexity to the gear and would only provide partial shielding. However, the shielding could be focused to address the greatest noise sources.

In contrast to the circular jet, the planar jet has received little examination in the literature and subject to a cross-flow, even less so. A book chapter by one of the authors [7] presents a summary of some of the research conducted [8–17] in order to advance the state of the art in air curtain knowledge, *viz.*, single and dual planar jets in a cross-flow from both a fluid mechanic and acoustic perspective. Analytical, numerical and experimental approaches have been adopted and used to validate each other.

An additional way to obtain a similar noise reduction is by adding small, locally mounted solid/perforated fairings [17, 18], meshes [19–21] or hub caps [22–25] to landing gear in order to improve the local aerodynamic shape or reduce local velocities, as well as some more advanced concepts such as; optimised bay door design [26], wheel bay treatments [23, 27, 28] and an upstream solid, retractable flow deflector [29–31]. A full review of noise reduction technologies for aircraft landing gear can be found in Zhao *et al.* [32] and a review of bio-inspired aerodynamic noise control in Wang *et al.* [33].

III. Simplified LAGOON Landing Gear Model

The original LAGOON LG was conceived in the 2000's to build an experimental database for the validation of Computational Aeroacoustics (CAA) techniques for airframe noise applications. The model represents a simplified version of a nose landing gear (NLG) or a direct main landing gear (MLG), and the base-line configuration consists of a profiled rod, a round main rod, a wheel axle and two wheels with inner rim cavities. The mock-up used in this paper is a simplified, down-scaled version of the LAGOON model, hereafter referred to as "LAGOON-SLG" (Fig. 2). This

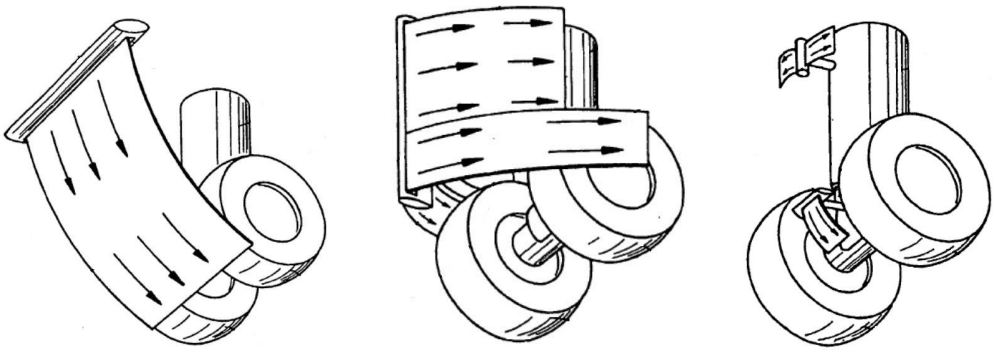

(a) Fuselage Mounted: Horizontal (b) Fuselage Mounted: Vertical (c) Landing Gear Mounted

Fig. 1 Air curtain concept for shielding landing gear (edited from [5])

model is scaled down to a wheel diameter of 0.15 m (hence having a 1:5 scale with respect to a real NLG) in order to minimise blockage effects in the wind tunnel facilities to be used. The cylindrical cavities on the inner side of the wheels, that produced unrealistic tones due to the appearance of Rossiter-type feedback-loop instabilities in the original LAGOON model, are in this research closed with flat covers. Additionally, the model is equipped with representative elements of an Airbus A320 MLG configuration such as a torque link allocated upstream of the main rod, and brake-like protuberances (Fig. 3) to reproduce most of the noise sources mimicking a real configuration. Furthermore, the profiled rod section, that was originally included in the LAGOON LG to minimise noise scattering due to the interaction between the wind-tunnel jet shear layer and the LG cylindrical rod is removed in the wind tunnel tests in this paper.

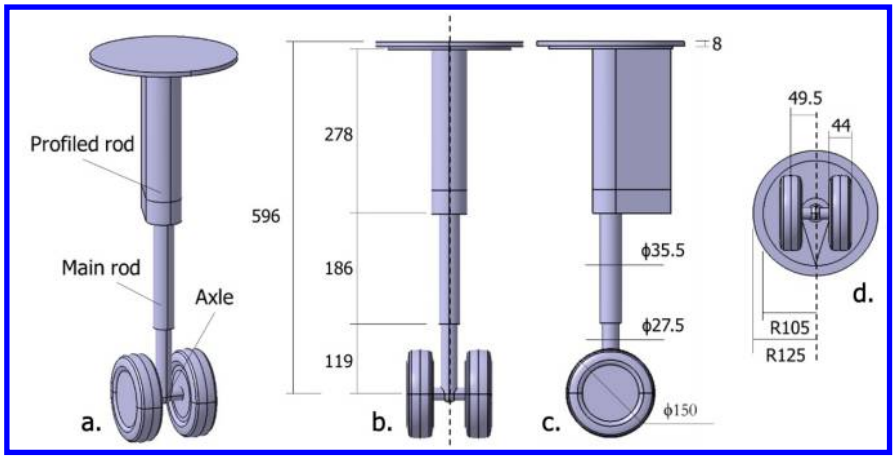

Fig. 2 Sketch of the LAGOON-SLG model in baseline configuration without brakes and torque-link (shown below). Distances in mm. (a) Isometric view (b) Front view (c) Side view (d) Bottom view.

IV. Experimental Assessment of Permeable Fairing Technology

The porous material experiments were conducted in the anechoic vertical wind tunnel (A-Tunnel) at Delft University of Technology (TU Delft). The A-tunnel is an open-jet closed-circuit facility with the test section located in an anechoic plenum with dimensions 6.4x6.4x3.2m^3. The model is placed horizontally with the wheel axle at the centre of the 40x70cm^2 nozzle exit (Fig. 4). The distance between axle and nozzle exit can be adapted to guarantee the correct localisation of noise sources of interest. A flat plate is flush mounted to the nozzle exit to mimic the aircraft wing (or fuselage belly). The model is attached to the tunnel with a turntable which allows to adjust the yaw angle.

The model is equipped with a mounting support for different types of flow-permeable fairings (Fig. 4). The mounting support is attached directly to the LAGOON-like model through the anchorage points at main rod and wheels.

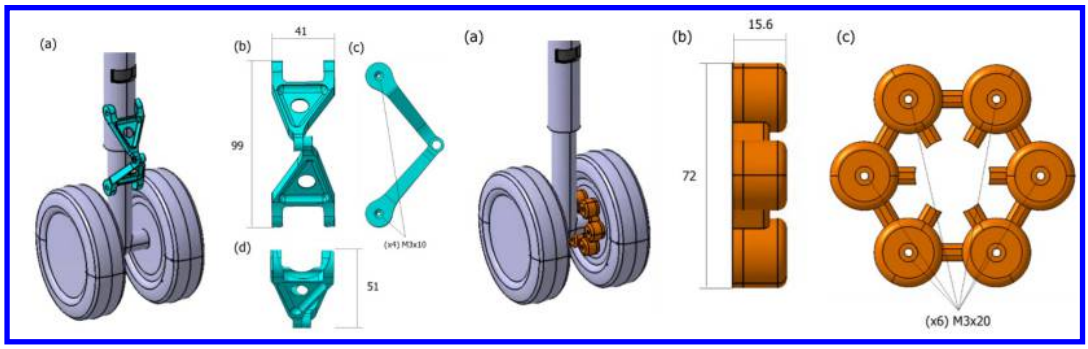

Fig. 3 Detail of the torque link (in light blue-left) and brakes (in orange left). Distances in mm. (a) Isometric view of assembly with baseline model (b) Front view (c) Side view (d) Top view.

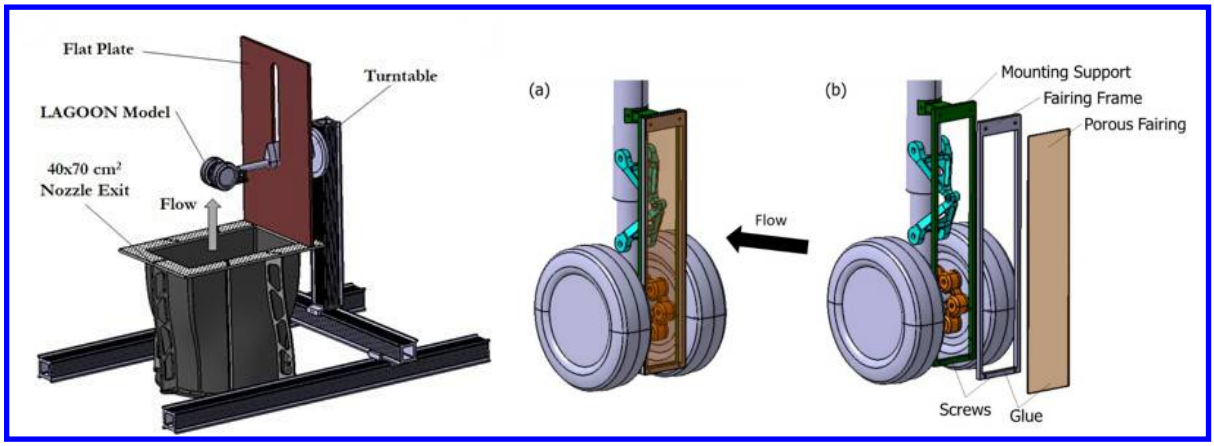

Fig. 4 Sketch of the experimental setup and detail of the mounting support (green), fairing frame (grey) and porous fairings (orange, translucid) installed on the baseline LAGOON-SLG model. (a) Isometric view (b) Exploded view. (a) Isometric view (b) Top view.

This configuration limits the presence of auxiliary struts (which might have a non-negligible effect on the resulting flow and acoustic fields), minimises vibrations, and it mimics the support in a real configuration. The mounting support allows to install flat porous fairings with dimensions of 54x270mm^2. The fairing covers wheel axle, brakes, torque link and the lower part of the main rod. The support allows to install porous panels with thickness of up to 10 mm. To facilitate the attachment of materials with different micro-structures and stiffen the fairing, every porous panel is attached to a light metallic frame. The frame is in turn screwed to the mounting support. The mounting support holds the porous fairing in-between the wheels and it allows to easily vary the distance between the main rod axis and the porous fairing. The minimum distance (55mm) is determined by the presence of the torque link (in this configuration the minimum distance be-tween torque link and fairing is 4mm), while the maximum (75mm) distance configuration is obtained by aligning the back of the fairing with the upfront of the wheels.

A. Flow field and Acoustic Measurements

Static pressure data over the main rod and wheels are obtained by means of pressure taps. The number of taps is limited by the availability of space to host the cabling inside the model. 20 pressure taps are allocated at the mid-span plane of the left-side (as seen from the back of the model) wheel along the entire circumference, with steps of 18 degrees (Fig. 5). The right wheel is instrumented with 3 pressure taps at locations 0, 1 and 19. These are employed to assess the symmetry of the set-up.

An additional 17 pressure taps were allocated in the main rod both axially and circumferentially. Data are available for comparisons but not presented in the current manuscript. Axial taps are within 50 and 70 mm away from the axle axis, with steps of 5 mm. Circumferential taps are distributed over the streamwise-vertical plane located 50 mm away from the axle. Taps are distributed among both stagnation points with steps of 12 degrees. Taps at 72 and 84 degrees

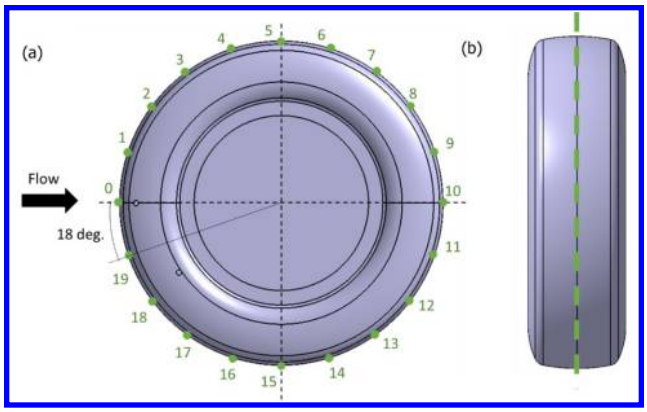

Fig. 5 Pressure tap distribution along left wheel. (a) Side view (b) Top view. Green dots indicate pressure taps.

are not included due to manufacturing constraints. The wake flow is characterised with Stereoscopic Particle Image Velocimetry (SPIV) on a vertical-spanwise cross-section, as well as a series of planar PIV measurements on different streamwise-spanwise planes (Fig. 6). The feasibility of characterising the flow around the porous fairing with PIV will be assessed. For cases where illumination or seeding were not satisfactory, hot-wire anemometry (HWA) was employed.

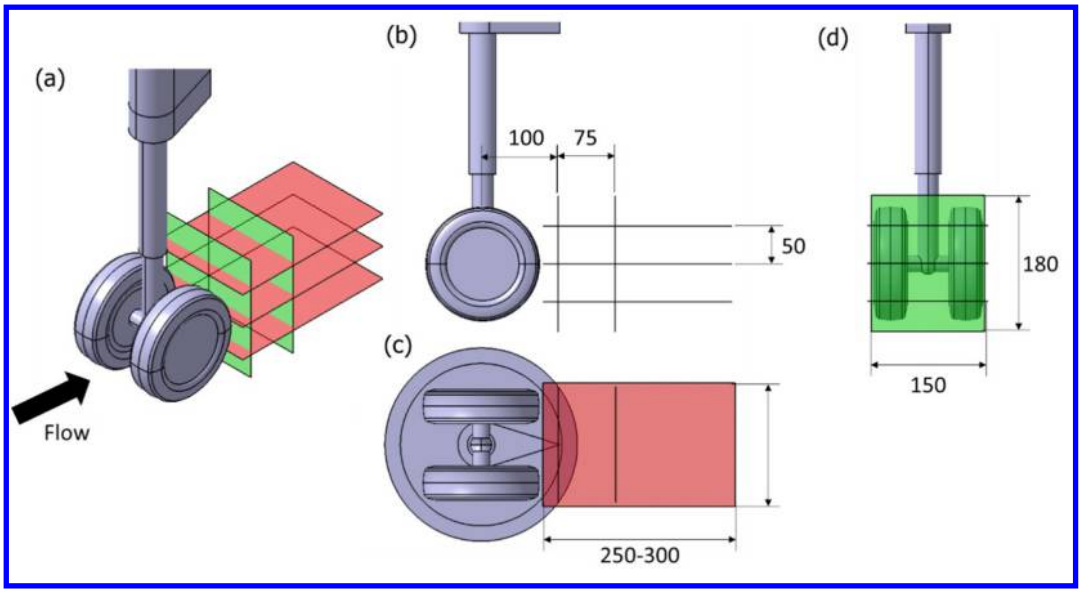

Fig. 6 Measurement planes for PIV. Green and red planes mark areas for 2D3C and 2D2C PIV fields-of-view respectively. Distances in mm. (a) Isometric view. (b) Side view. (c) Bottom view. (d) Back view.

Acoustic measurements are carried out with a 2x1m^2 microphone antenna comprising 64 40PH G.R.A.S. microphones. The antenna is placed 1.5 meters away from the model, and data are obtained with the array in a “flyover" configuration, i.e. with the array looking at the bottom of the LAGOON-SLG. Additional measurements with the antenna looking from the side might be performed on the configurations regarding the torque link. These setups allow to retrieve absolute far-field noise levels, as well as to localise and isolate noise generation at different regions within the model. Measurements are performed at Mach numbers of 0.04, 0.07 and 0.1, corresponding to free-stream velocities of 15, 25 and 35m/s.

B. Flow visualization of the baseline configuration

The first results concern the mean flow of the baseline configuration consisting of the landing gear with torque link and brakes. Streamline and spanwise velocities are shown in Fig. 7 from which it can be seen that the main wheel

region creates a substantial higher separation with respect to the rod. Analysis of the instantaneous PIV snapshots and further investigation of the turbulent intensity and in-plane Reynolds stresses in Fig. 8 shows a considerable shedding from both the rod and the wheels region, building up the final momentum deficit in the back of the structure.

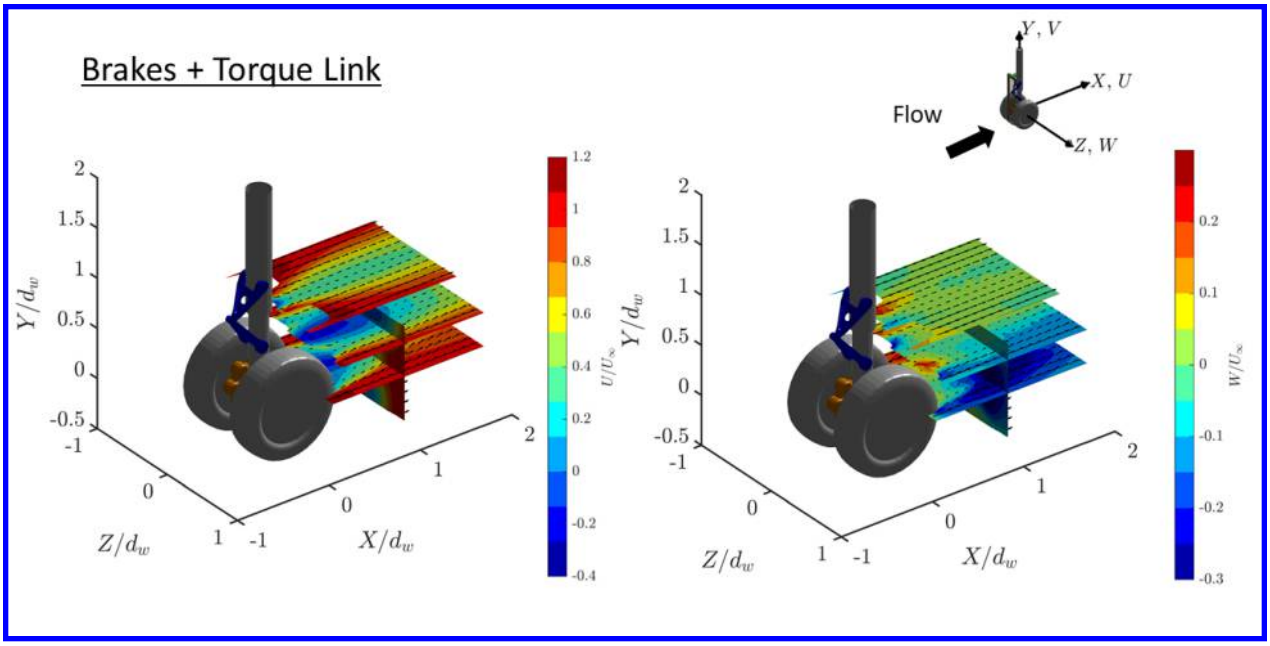

Fig. 7 Magnitude of mean streamwise and spanwise velocity from particle image velocimetry planes. Legend and reference system as indicated in top right.

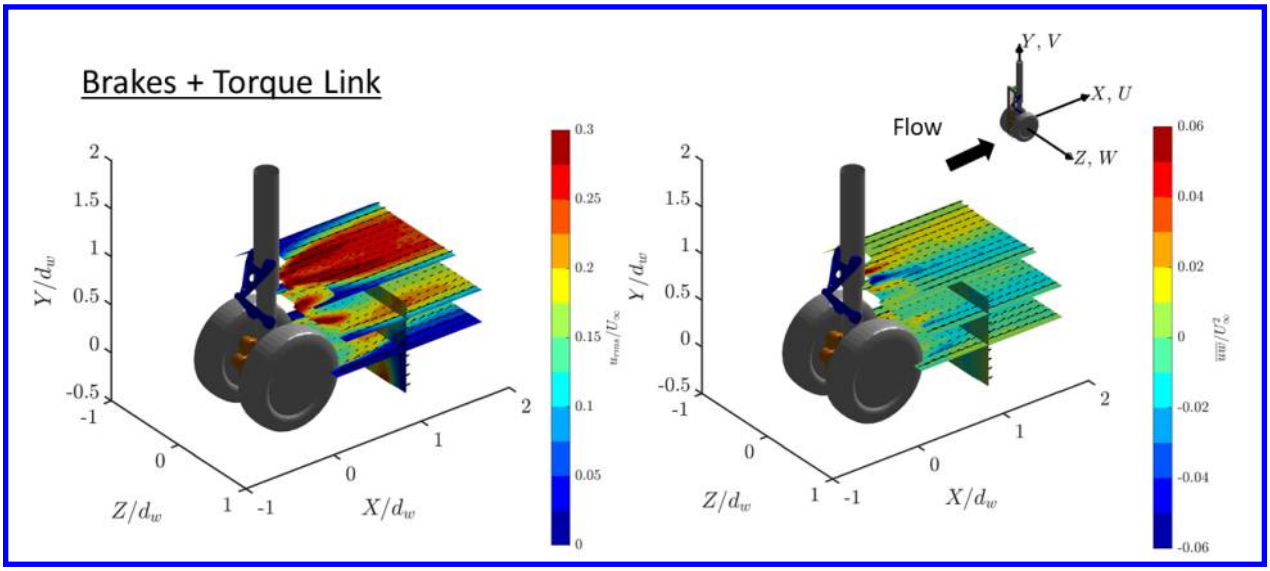

Fig. 8 Turbulent intensity and in-plane Reynolds stresses from PIV planes. Legend and reference system as indicated in top right.

C. Acoustic response of solid and porous fairings

The acoustic response of the solid and porous fairings is assessed from the microphone data in flyover conditions. As anticipated several fairing configurations have been tested, including porous materials, wire-meshes and modular 3d-printed cells. In the present study, only results from the TU Delft porous diamond lattice with different cell-size will

be reported for Confidentiality reasons. In the first assessment in Fig. 9 the LAGOON-SLG configuration is tested in the the baseline form, with brakes and torque link. As it can be seen the acoustic response shows a narrow-band peak, centred at shedding frequencies of the landing gear. A first fully solid fairing (i.e. fairing with no possibility for the flow to permeate through), is tested. The acoustic response shows that the solid fairing is able to break the shedding mechanism and to deliver with a lower noise footprint that the original configuration. The present result is consistent with what found in previous literature ([24, 34]); however, due to solid surface exposed to the flow, this configuration offers with the maximum loading to the landing structure. Therefore, the usage of porous materials is proposed with the aim to obtain a compromise between the noise-reduction performance and the actual loading on the landing gear structure.

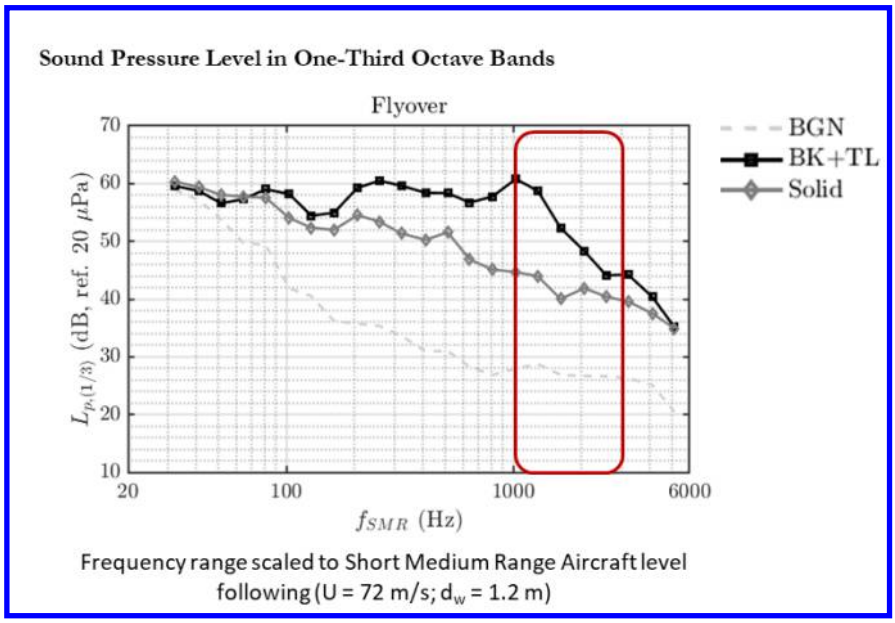

Fig. 9 Sound pressure level in one-third octave bands for baseline LAGOON-SLG configuration with brake and torque link, and with solid fairing.

Amongst all the materials that have been tested, in Fig. 10 a first study with respect to the cell-size (thus flow permeability) is carried out. The diamond lattice that has been used has been benchmarked by TU Delft already in studies for trailing edge noise [35], and it is used in this specific work as one of the materials that can be later accurately reproduced by high-fidelity simulations. As it can be seen from the results, all diamond lattice fairing provide with a positive noise reduction in the low frequency range. However, in the range of frequencies investigated for Short-Medium Range Aircraft Level, the unit cells which determine more resistance to the flow provide with better results, very close to the solid configuration, still allowing for flow to pass through the material and reduce the landing gear resistance. Within the INVENTOR project, a specific assessment of the degree of flow permeation with respect to noise reduction is carried out, and additional porous materials are compared to verify the actual performance with respect to the solid configuration.

V. Air Curtain Numerical Simulations

In order to help design the air curtains for the AWB wind tunnel tests, numerical simulations using ANSYS Fluent were conducted in advance. Initially, the analysis was conducted on the classic LAGOON model as provided by ONERA. This model is reported by research by Manoha *et al.* [3,4] and Saunders *et al.* [5] and has a wheel diameter of 300mm. These initial ANSYS results showed that a mass flow requirement for the air curtains in excess of that available in the AWB would be necessary. Hence, a second set of analyses were performed on the LAGOON model with a wheel diameter of 100mm. As the decision to experimentally assess the "LAGOON-SLG" (D=150mm) was made quite soon before the AWB test campaign, no numerical simulations were performed on that model but instead, numerical results from the 100mm LAGOON model were used to best inform the air curtain design.

In addition to the flow-field (CFD) analysis performed around the 300mm and 100mm LAGOON model and air

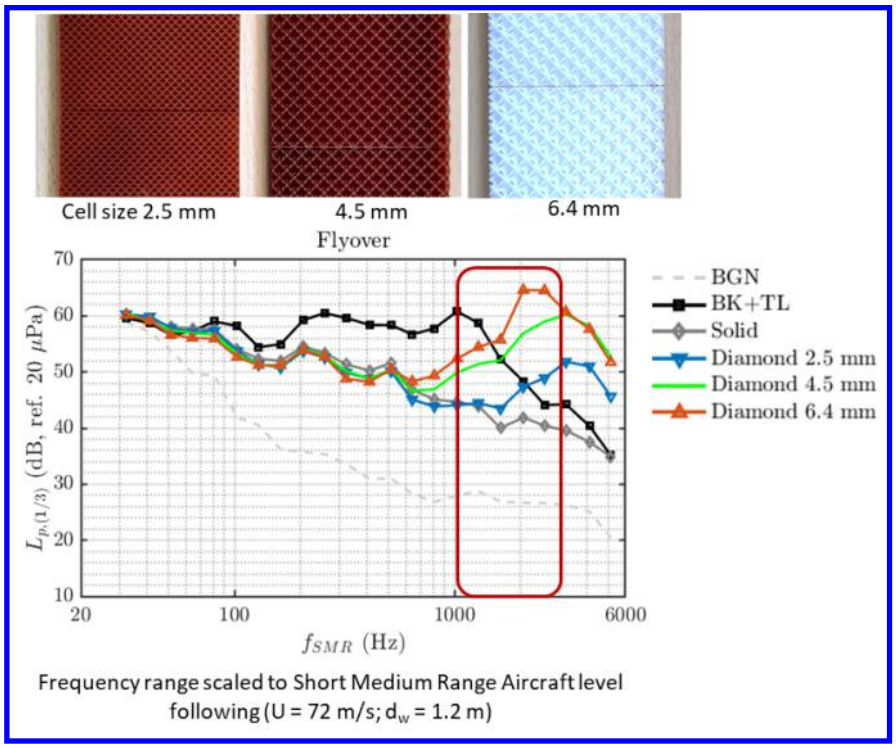

Fig. 10 Comparison of sound pressure level in one-third octave bands for baseline LAGOON-SLG configuration with brake and torque link, and with permeable diamond cell fairings.

curtains, some acoustic results were also obtained using a coupled CAA scheme using the FW-H acoustic analogy. The parameters for the analysis are given in Fig. 11. The domain and surface was finely meshed, with a y^+ value close to 1.

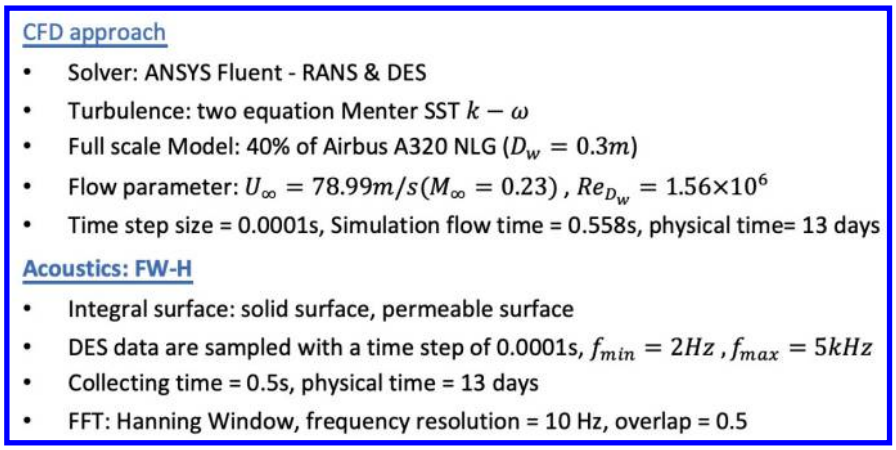

Fig. 11 CAA settings for ANSYS-Fluent analysis of the air curtains.

Figure 12, shows some baseline flow field and surface pressure results for the wheel diameter=300 mm and Fig. 13 provides a solution for a strut type air curtain similar to that shown in Fig. 1(b). In this example, the strut is split along its height with a lower velocity (V_1) issuing from the top section of the air curtain. This strategy is used to save air flow as not such a high velocity is needed to shield the leg which is narrower than the wheel section. The solution in Fig. 12 shows that when the air curtain is activated the landing gear is located in its lee and is shielded from the mean flow.

Figure 14 shows some air curtain solutions similar to Fig. 1(c) implemented on the LAGOON model with the smaller diameter, D=100mm. The *lac-a1* air curtain is located between the wheels with two air curtains issuing both up and down to shield the mid-wheel section from the mean-flow. *Lac-a2* is similar but is brought further upstream and is

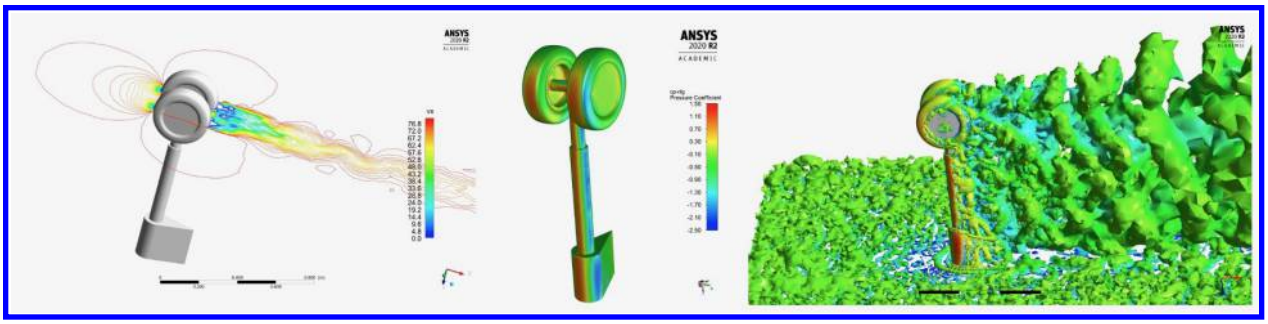

Fig. 12 Flow-field results for LAGOON D=300mm

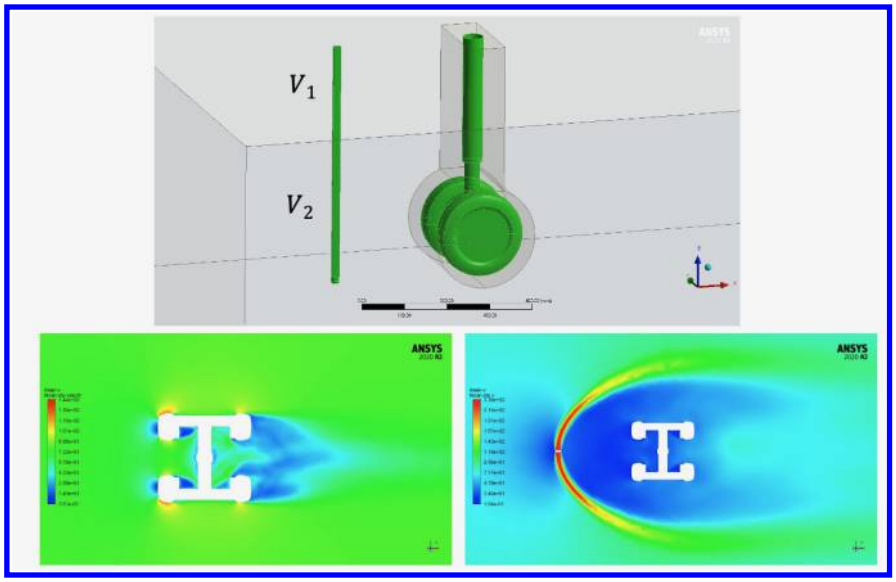

Fig. 13 Multiple Velocity Air curtain (MVAC) result with LAGOON D=300mm

wider to allow it to shield not only the mid-wheel section but also the wheels themselves. In the *lac-3* configuration we see that *lac-a1* is partnered with a leg mounted air curtain pair, *lac-b*, which will shield the leg from the mean-flow and also, potentially, from the *lac-a1* air curtain itself. We will also use this leg mounted air curtain to shield the LAGOON-SLG torque-link. Also to be noted is that it can be seen that *lac-a1* air curtain pair is similar to a "wind-shield" fairing which was evaluated in a different EU funded project ALLEGRA [25, 36] and found to be very effective.

VI. Mechanical Design and Implementation of Air Curtain Technology

As discussed, although the AC numerical analysis examined the LAGOON NLG, it was decided that the AC experimental campaign should focus on the LAGOON-SLG. This was not seen as an obstacle as the lessons learned from the numerical analysis could be applied to the similar set-up. Accordingly, the LAGOON-SLG CAD which was designed by TU Delft was received by TCD and used at the same scale, i.e. a wheel diameter of D=150mm. The CAD was modified to facilitate manufacture and 3D printing and to allow it to be securely mounted to the flat wooden plate which will form one side of the 3/4 open-jet set-up to be found in the AWB wind tunnel, this installation differing from that in the TU Delft ATunnel. Based on the numerical analysis, only locally mounted air curtains were considered due to air flow limitations at this scale.

Figures 15 and 16 show the CAD designs of the air curtain solutions as applied to the LAGOON-SLG. Two versions of the air curtains are used to shield the wheels and brakes, while another mounted to the leg will shield the torque link. The design allows for easy substitution of the air curtains with differing variations and blanking plates have been designed to allow for a baseline configuration to be assessed without air curtain fixtures present.

Figure 17 shows the manufactured realisation of the CAD designs. Aluminium was chosen to manufacture the leg in

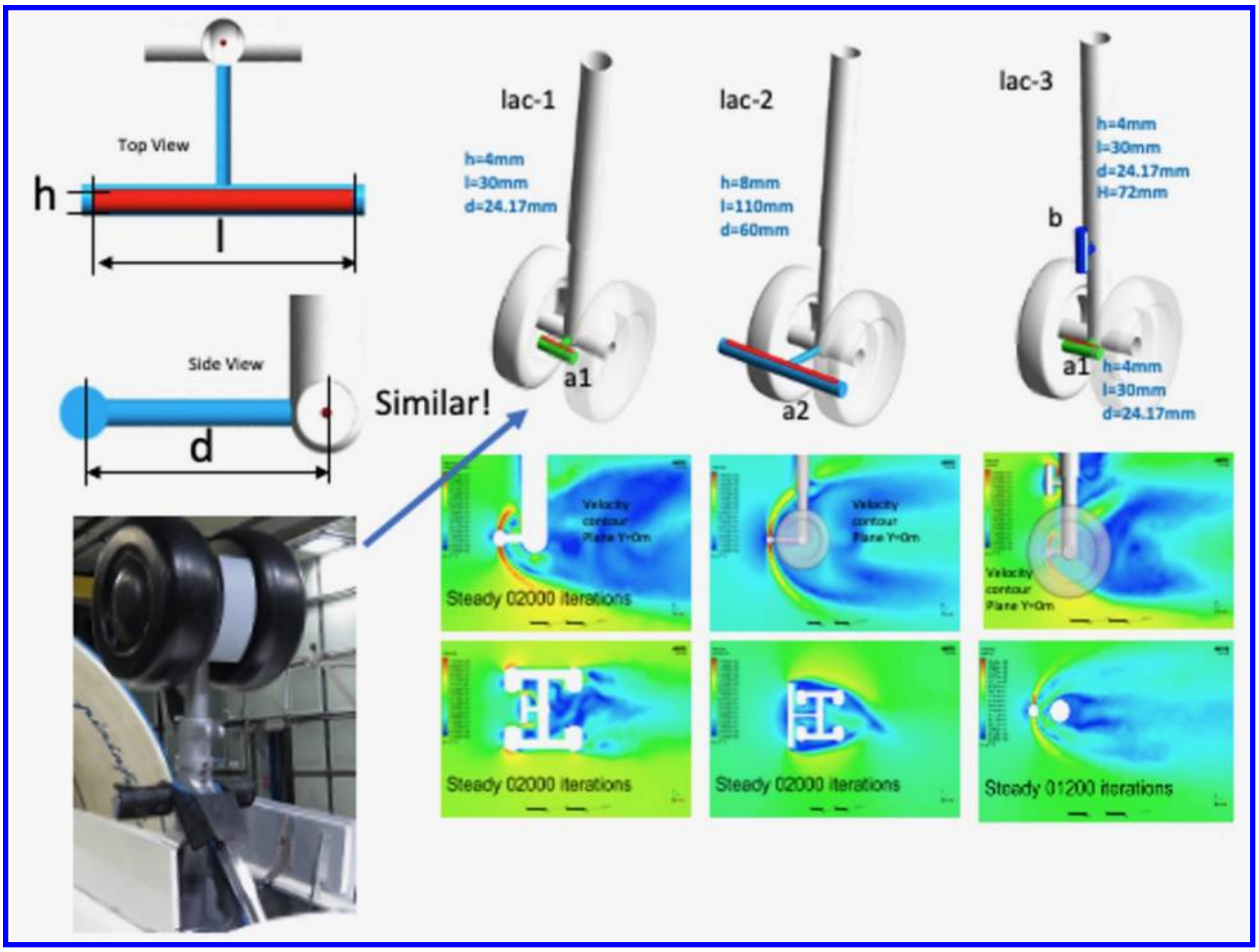

Fig. 14 Local air curtain (lac) solutions mounted to LAGOON D=100mm

order to withstand the aerodynamic loading at 60 m/s whereas the wheels, air curtains and attachments, the torque link and the wheel/leg junction were 3D printed. In the images, all orange components were 3D printed with a Prusa SL1, masked stereolithography (MSLA) 3D printer using a UV photo-sensitive resin (Prusament Tough Orange). A 100 micron step size was used. Threaded brass inserts were push-fit into the resin parts to allow for assembly. The yellow wheels were printed with a Prusa i3 MK3 Fused Deposition Modelling (FDM) 3D printer. FDM was used for the wheels as they are too big for the build plate of the SL1 and also the resolution is sufficient. Masking tape and blanking plates was used to cover any holes prior to wind tunnel testing. The default air curtain width is 2mm with a 3mm wall thickness. However, these are designed to be removable to allow other parameter permutations to be tested. For example, a 4mm slot width was also tested and by changing the wall thickness, the chamber volume within was altered which affects the velocity exit profile. A number of other air curtains with these alternative parameters were been printed and will be examined during the test campaign.

VII. Experimental Assessment of Air Curtain Technology

The wind tunnel tests for the air-curtains took place in the Aeroacoustic Wind Tunnel Braunschweig (AWB) which is DLR's small, high-quality test facility for aeroacoustic noise measurements. The facility is an open jet, closed circuit tunnel, with the test section located in an anechoic plenum with dimensions of approximately $8x8x5m^3$. The facility was upgraded both aerodynamically and acoustically, as described in a publication by Pott-Polenkse and Delfs [37] and can achieve 60 m/s from a 0.8 m X 1.2 m nozzle. A plan view of the facility is given in Fig. 18(a) with a view of the nozzle and collector shown in Fig. 18(c) and Fig. 18(b) respectively.

The tunnel was instrumented with two microphone arrays at sideline and overhead positions complete with 48 and

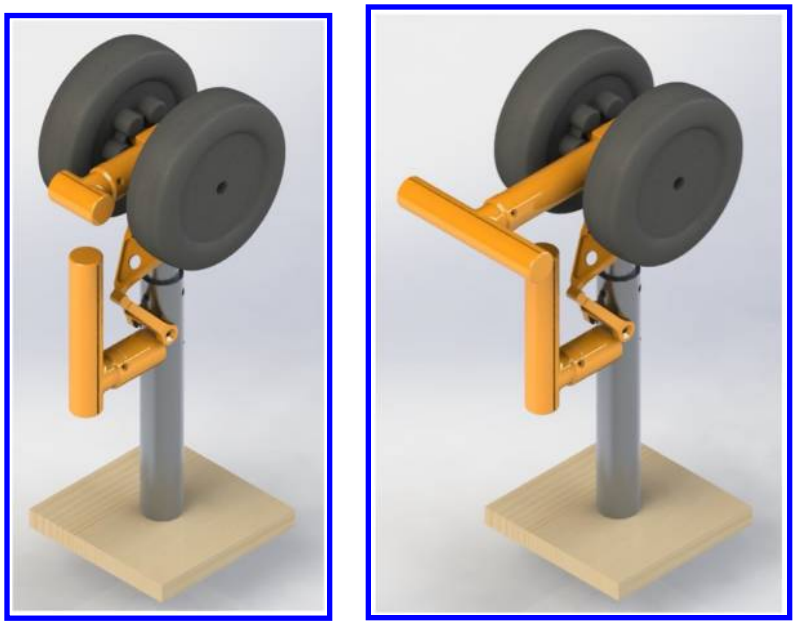

(a) LAGOON-SLG. D=150mm. Lac a1 and Lac b.

(b) LAGOON-SLG. D=150mm. Lac a2 and Lac b.

Fig. 15 Air curtain designs for shielding the LAGOON-Like LG.

(a) LAGOON-SLG. D=150mm. Exploded view.

(b) LAGOON-SLG. D=150mm. Side view showing mounting plates.

Fig. 16 Details of the model and its installation.

96 microphones respectively. Data from the array microphones was sampled at 100 kHz applied with a 500 Hz high pass filter. In addition, 6 X 1/4 inch condenser microphones were located at sideline and overhead positions to calculate directivity spectra. These microphones were also sampled at 100 kHz with no filtering applied. Three wind tunnel test speeds were applied: 31.5 m/s, 50 m/s and 63 m/s. It is to be noted that the maximum velocity tested here is less than that in the TU-Delft A-Tunnel at 72 m/s. The compressed air supply for the air curtains was provided by a large on-site

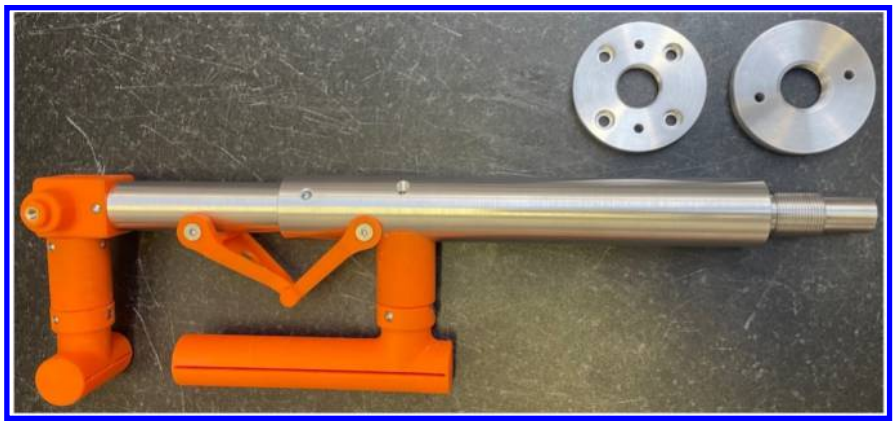

(a) Leg, mounting plates and 3D printed torque-link, Lac a1 and Lac b.

(b) A single wheel with brakes is shown.

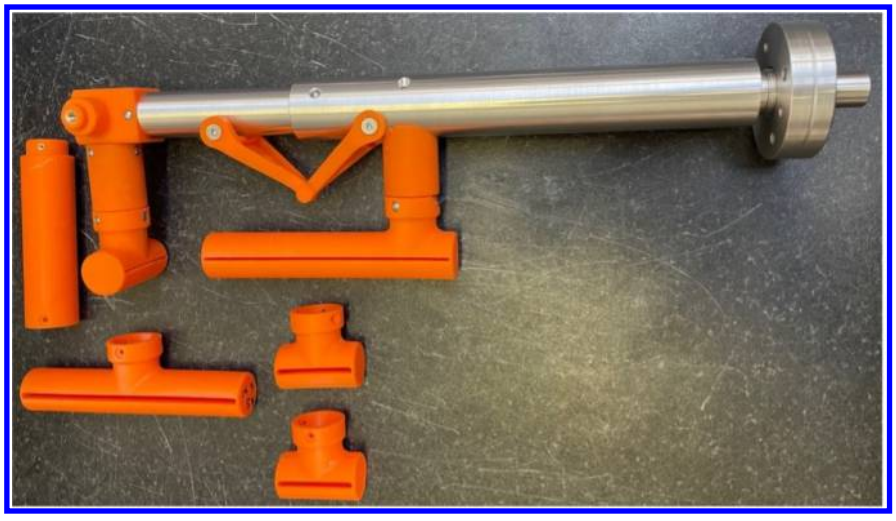

(c) Lac a1, a2 and b are shown in addition to other variations.

Fig. 17 LAGOON-SLG manufactured. Silver parts are machined aluminium. Orange parts are MSLA 3D printed from UV photosensitive resin. Yellow wheels and brakes are FDM 3D printed from PLA filament.

compressor with the maximum flow rate achievable being 0.04 m^3/s.

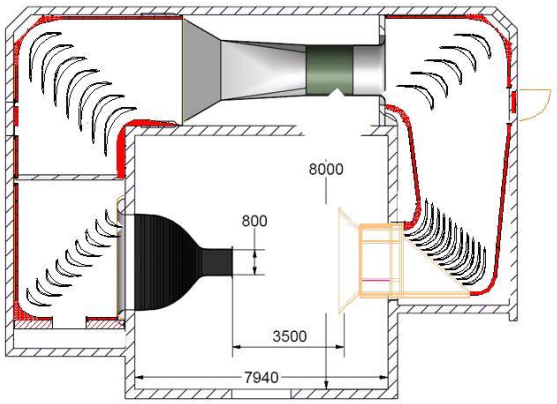

(a) AWB: Plan View

(b) AWB: Collector

(c) AWB: Nozzle with collector

Fig. 18 Aeroacoustic Wind Tunnel (AWB) at DLR Braunschweig

Figure 19(a) shows the baseline Lagoon-SLG model installed in the AWB wind tunnel, with Figs. 19(b), 19(c) and 19(d) showing the three main air curtain configurations tested.

Figure 20(a) shows a typical result from the test campaign. At this low wind tunnel speed, the noise generated from this small NLG is very low: 50 dB - 30 dB. When there is flow from the air curtain nozzle, the Lac a1 type in Fig. 19(b) in this case, the noise it generates itself far exceeds that of the landing gear. When the air tunnel is turned on, the noise level increases yet again.

In Fig. 20(b) the sideline beamforming view of this test case can be seen when the tunnel is turned on with the nozzle turned off. It must be pointed out that the background image indicates the presence of the Lac b nozzle but it is was not attached for this test. The background image is just the general image for all test cases to help relate the beamforming result to the landing gear location. In the beamforming plot, we see the maximum noise source to be located for of the torque link with possible noise contributions coming from between the wheels and from the brakes. The level is 54 dB. When the air curtain nozzle is turned on, the noise source location moves to the nozzle location itself with an increase in noise level to 84 dB. Similar results were found at the sideline position and for the other air curtain types and locations. For higher wind tunnel speeds, as seen in Fig. 21, the noise levels from the Lagoon-SLG model are higher: 70 dB - 50 dB and so the relative increase in noise from the nozzles, which remains constant is not so great. In Fig. 21, at the higher tunnel velocity, the affect of the air curtain for low frequencies is to reduce the landing gear noise or to have no impact. We see that between 1 kHz and 3 kHz however, similar to the results with the porous materials in Fig.

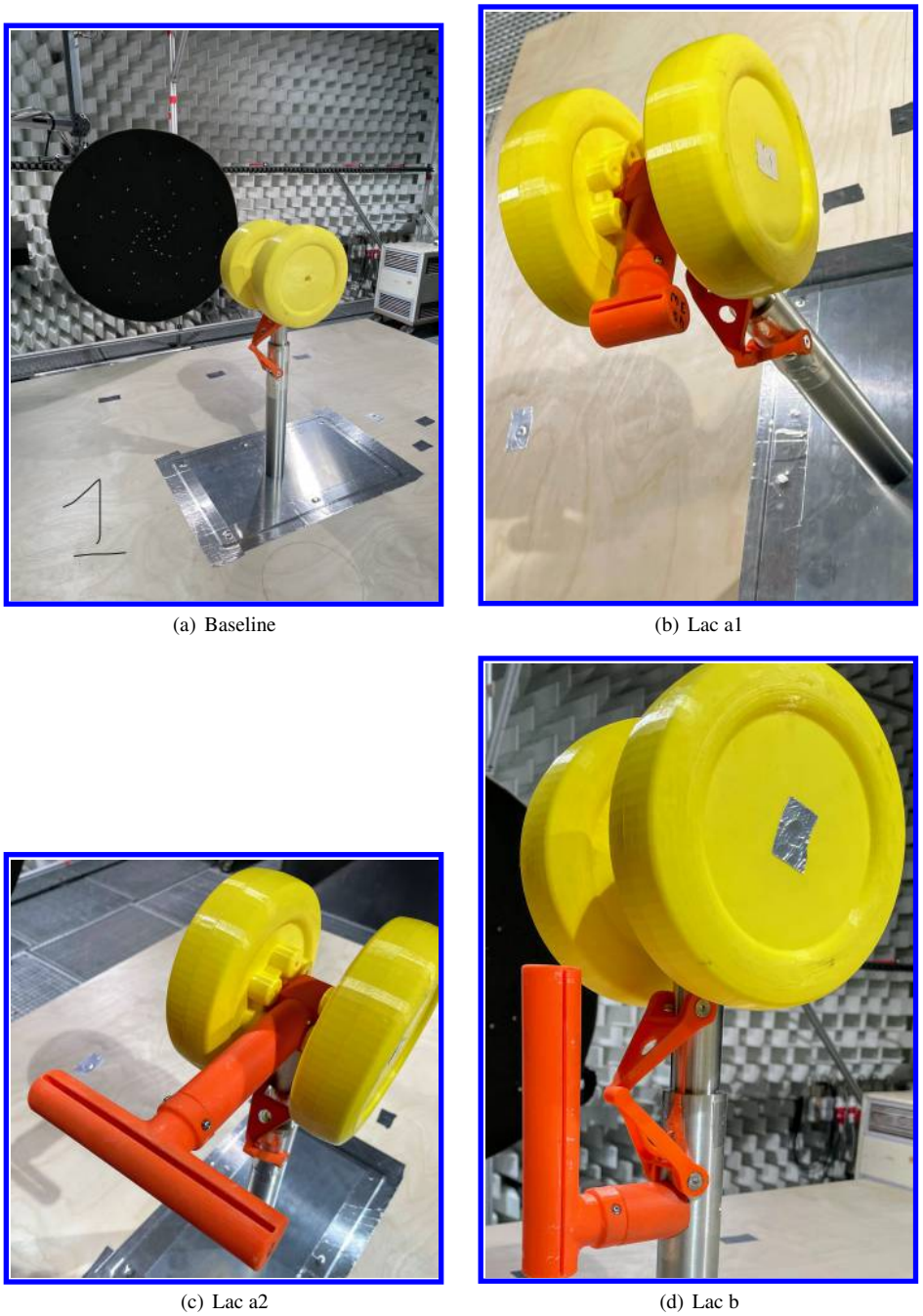

(a) Baseline (b) Lac a1

(c) Lac a2 (d) Lac b

Fig. 19 Lagoon-SLG D=150mm in situ in AWB

10, the presence of the air curtain is to increase the net noise level which is counter to the objectives of the air curtains.

For the test campaign, most effort was expended in preparing the tunnel, compressed air supply, the manufacture of the Lagoon-SLG model and the correct location of the air curtain outlets. However, little effort was spent in the design of the nozzles themselves which clearly generate excess noise in themselves.

In order, to try and demonstrate the proof of concept, the baseline Lagoon-SLG model was modified to be louder through the addition of a short length of pipe to create a whistling tone. In parallel a new air curtain similar in shape to Lac b was constructed in copper in the AWB workshop. The outlet nozzles were fitted with a fine mesh and the final installed design can be seen in Fig. 22. The resuts from this new test set-up can be seen in Fig. 23. Fig. 23(a) shows

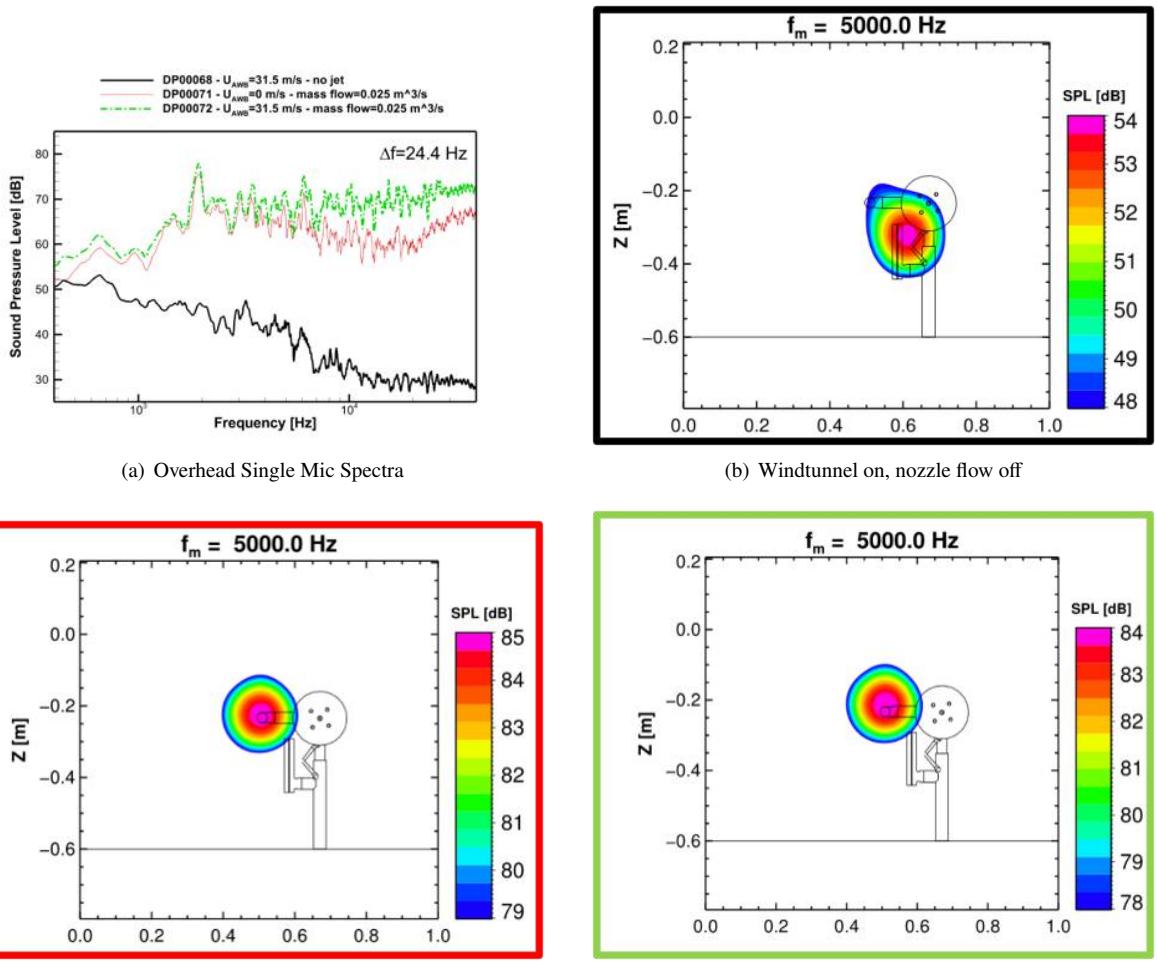

(a) Overhead Single Mic Spectra

(b) Windtunnel on, nozzle flow off

(c) Windtunnel off, nozzle flow on

(d) Windtunnel on, nozzle flow on

Fig. 20 AWB spectra and beamforming results. Lagoon-SLG, D=150mm, V=31.5 m/s, Lac a1

the spectra of the modified baseline with a new tone being generated at approx. 4.2 kHz which is suppressed with the addition of flow from the air curtain. This is certainly an artificial situation and it should be noted that the active air curtain increases the noise level above that of the whistling landing gear at all frequencies except at the tone. However, the air curtain self noise has been significantly reduced over the previous design and it successfully eliminated a noise source of greater amplitude. This exercise has shown that there is scope to reduce the self noise of the air curtain itself and that it can be implemented to reduce landing gear noise.

VIII. Conclusions

Air Curtains The air curtain concept has been demonstrated numerically for the first time with realistic landing gear, in this case the Lagoon NLG. The air curtain redirects the upstream flow creating a fluid shield which places the landing gear in its lee and reduces the aerodynamic noise. A modified Lagoon NLG, called the LAGOON-SLG was developed with brakes and a torque link and was manufactured and tested in the DLR, AWB wind tunnel. A variety of air curtains were 3D printed to reduce noise sources at the wheel and torque link locations. Compressed air was supplied from a separate compressor at the AWB facility and a parametric analysis was performed assessing each combination of air curtains. For velocities close to air craft approach, the results seem to indicate that the air curtains can be effective below a range between 1 kHz and 3 kHz but above that range they increase the overall noise. Further work is required to redesign the air curtains to reduce their self noise. Preliminary results are promising.

Permeable Fairing Technology In the project INVENTOR a series of flow-permeable materials have been tested in

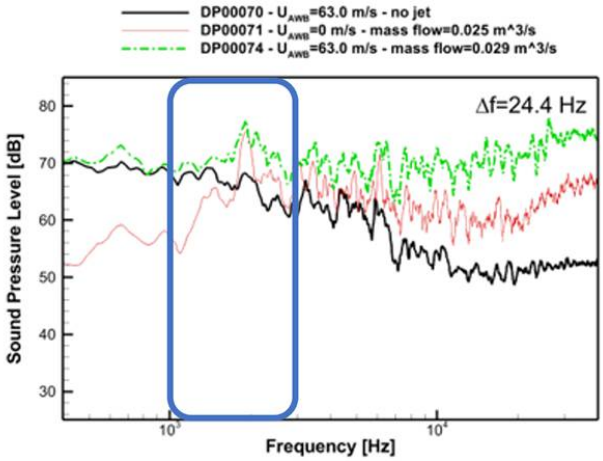

Fig. 21 Modified Lac b air curtain with whistling Lagoon-SLG model.

Fig. 22 Modified Lac b air curtain with whistling Lagoon-SLG model.

a fairing frame, with the aim of finding the best compromise between noise reduction performance and extra loading on the structure. The conventional usage of a very blunt solid fairing is found to postpone the shedding downstream of the landing gear, changing the flow pattern and reducing the effect of the flow instability on the noise. However, the loading created by the increase surface exposed flow can be reduced by using porous fairings, which allow to reduce the exposed drag still preserving the noise reduction characteristics. In the project INVENTOR several materials including wire-meshes and modular open cells have been tested. Although covered by Confidentiality reasons, results seem to point out that a relation between the effectiveness of the noise reduction versus its frequency can be drafted with respect to the unit-cell. The full bench-mark will be published in conjunction with the participating institutes.

Acknowledgements

This project, INVENTOR, has received funding from the European Union's Horizon 2020 research and innovation programme under grant agreement No 860538.

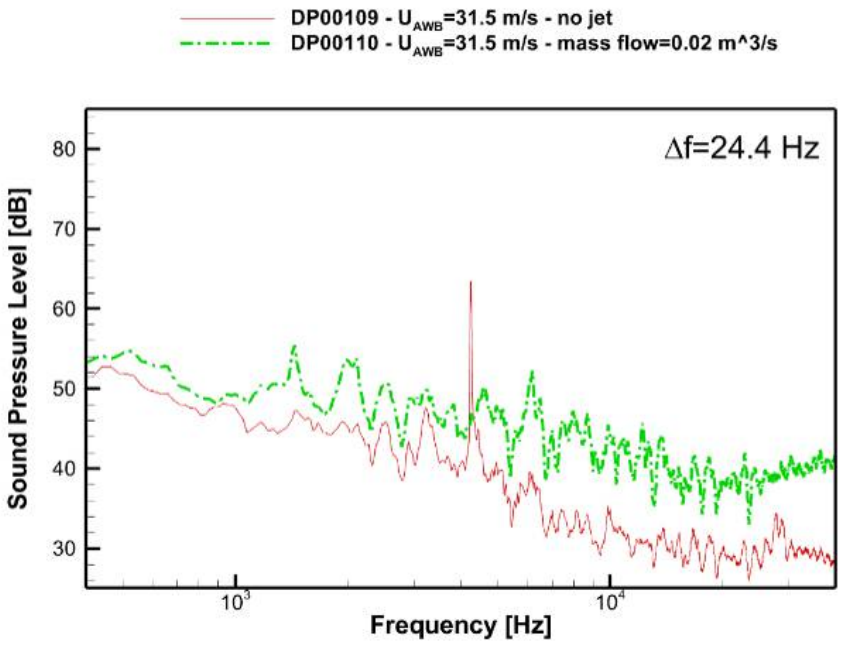

(a) Overhead spectra

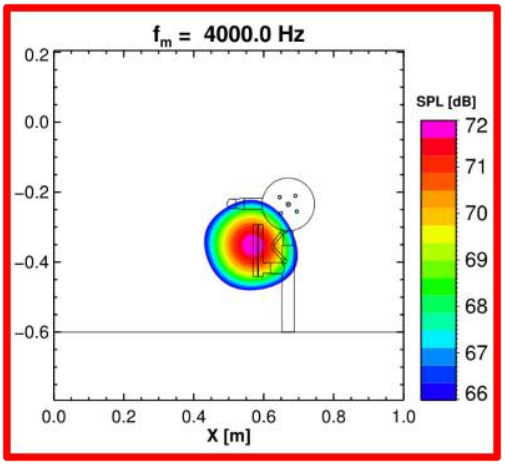

(b) Windtunnel on, nozzle flow off

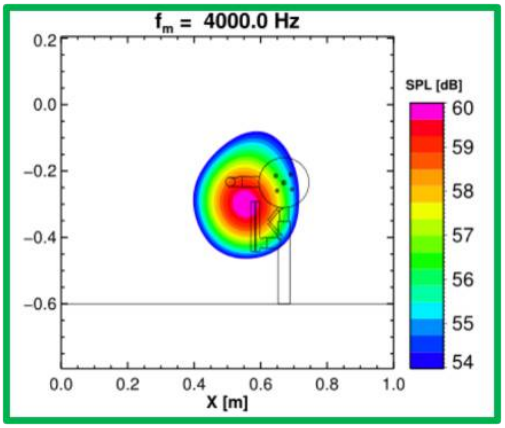

(c) Windtunnel on, nozzle flow on

Fig. 23 AWB spectra and beamforming results. Lagoon-SLG, D=150mm, V=31.5 m/s, Modified Nozzle

References

[1] Guyonnaud, L., Solliec, C., de Virel, M. D., and Rey, C., "Design of air curtains used for area confinement in tunnels," *Experiments in Fluids*, Vol. 28, No. 4, 2000, pp. 377–384. doi:10.1007/s003480050397.

[2] Hu, L., Zhou, J., Huo, R., Peng, W., and Wang, H., "Confinement of fire-induced smoke and carbon monoxide transportation by air curtain in channels," *Journal of hazardous materials*, Vol. 156, No. 1, 2008, pp. 327–334. doi:10.1016/j.jhazmat.2007.12.041.

[3] Navaz, H. K., Henderson, B. S., Faramarzi, R., Pourmovahed, A., and Taugwalder, F., "Jet entrainment rate in air curtain of open refrigerated display cases," *International Journal of Refrigeration*, Vol. 28, No. 2, 2005, pp. 267–275. doi: 10.1016/j.ijrefrig.2004.08.002.

[4] Huang, R. F., and Chou, C. I., "Flow and performance of an air-curtain biological safety cabinet," *The Annals of occupational hygiene*, Vol. 53, No. 4, 2009, pp. 425–40. doi:10.1093/annhyg/mep020, URL http://www.ncbi.nlm.nih.gov/pubmed/19398506.

[5] Sijpkes, T., and Wickerhoff, J., "Aeroplane provided with noise-reducing means, as well as a landing gear and blowing means," , June 2004. The US Patent 20040104301 A1.

[6] Oerlemans, S., and De Bruin, A., "Reduction of landing gear noise using an air curtain," *15th AIAA/CEAS Aeroacoustics Conference (30th AIAA Aeroacoustics Conference)*, 2009. doi:10.2514/6.2009-3156.

[7] Bennett, G. J., and Zhao, K., "Air Curtain Flow Control for Aerodynamic Noise Reduction," *Fundamentals of High Lift for Future Civil Aircraft*, Vol. 145, edited by R. Radespiel and R. Semaan, Springer International Publishing, Cham, 2021, pp. 279–295. doi:10.1007/978-3-030-52429-6_18, URL http://link.springer.com/10.1007/978-3-030-52429-6_18, series Title: Notes on Numerical Fluid Mechanics and Multidisciplinary Design.

[8] Zhao, K., Yang, X.-x., Okolo, P. N., Zhang, W.-h., and Gareth J. Bennett, "Use of a plane jet for flow-induced noise reduction of tandem rods," *Chinese Physics B*, Vol. 25, No. 6, 2016, pp. 064301–1 – 064301–9. doi:10.1088/1674-1056/25/6/064301, URL http://stacks.iop.org/1674-1056/25/i=6/a=064301?key=crossref.b90e51e4f1a72600400a9f694ec0b0af.

[9] Zhao, K., Okolo, P. N., Kennedy, J., and Bennett, G. J., "2D PIV measurement on the interaction zone between two parallel planar jets in a crossflow," *AIP Advances*, Vol. 7, No. 10, 2017, pp. 105104–1 – 105104–21. doi:10.1063/1.5005017, URL http://aip.scitation.org/doi/abs/10.1063/1.5005017.

[10] Zhao, K., Yang, X., Okolo, P. N., Wu, Z., Zhang, W., and Bennett, G. J., "A Novel Method for Defining the Leeward Edge of the Planar Jet in Crossflow," *Journal of Applied Fluid Mechanics*, Vol. 10, No. 5, 2017, pp. 1475–1486. doi:10.18869/acadpub.jafm.73.242.27617, URL http://jafmonline.net/JournalArchive/download?file_ID=43345&issue_ID=242.

[11] Zhao, K., Yang, X., Okolo, P. N., Wu, Z., and Bennett, G. J., "Use of dual planar jets for the reduction of flow-induced noise," *AIP Advances*, Vol. 7, No. 2, 2017, pp. 025312–1 – 025312–7. doi:10.1063/1.4976336, URL http://aip.scitation.org/doi/10.1063/1.4976336.

[12] Zhao, K., Alimohammadi, S., Okolo, P. N., Kennedy, J., and Bennett, G. J., "Aerodynamic noise reduction using dual-jet planar air curtains," *Journal of Sound and Vibration*, Vol. 432, 2018, pp. 192–212. doi:10.1016/j.jsv.2018.06.036, URL https://linkinghub.elsevier.com/retrieve/pii/S0022460X18303985.

[13] Zhao, K., Okolo, P. N., Wang, Y., Kennedy, J., and Bennett, G. J., "An Experimental Characterization of the Interaction Between Two Tandem Planar Jets in a Crossflow," *Journal of Fluids Engineering*, Vol. 140, No. 11, 2018, pp. 111106–1 – 111106–12. doi:10.1115/1.4040224, URL http://fluidsengineering.asmedigitalcollection.asme.org/article.aspx?doi=10.1115/1.4040224.

[14] Gareth J. Bennett, Kun Zhao, John Philo, Yaoyi Guan, and Scott C. Morris, "Cavity Noise Suppression Using Fluidic Spoilers," *22nd AIAA/CEAS Aeroacoustics Conference*, American Institute of Aeronautics and Astronautics, Lyon, France, 2016. doi:10.2514/6.2016-2756, URL http://arc.aiaa.org/doi/10.2514/6.2016-2756.

[15] Gareth J. Bennett, Patrick N. Okolo, Kun Zhao, John Philo, Yaoyi Guan, and Scott C. Morris, "Cavity Resonance Suppression Using Fluidic Spoilers," *AIAA Journal*, Vol. 57, No. 2, 2018, pp. 706–719. doi:10.2514/1.J057407, URL https://arc.aiaa.org/doi/10.2514/1.J057407.

[16] Kun Zhao, Patrick N Okolo, John Kennedy, and Gareth J Bennett, "A study of planar jet flow control and perforated fairings for the reduction of the flow-induced noise of tandem rods in a cross-flow (AIAA2016-2772)," *22nd AIAA/CEAS Aeroacoustics Conference*, AIAA, Lyon, France, 2016. doi:10.2514/6.2016-2772, URL http://arc.aiaa.org/doi/10.2514/6.2016-2772.

[17] Zhao, K., Liang, Y., Okolo, P. N., Wang, Y., Wu, Z., and Bennett, G. J., "Suppression of aerodynamic noise using dual-jet air curtains combined with perforated fairings," *Applied Acoustics*, Vol. 158, 2020, p. 107042. doi:10.1016/j.apacoust.2019.107042, URL https://linkinghub.elsevier.com/retrieve/pii/S0003682X19301793.

[18] Boorsma, K., Zhang, X., Molin, N., and Chow, L. C., "Bluff Body Noise Control Using Perforated Fairings," *AIAA Journal*, Vol. 47, No. 1, 2009, pp. 33–43. doi:10.2514/1.32766, URL http://dx.doi.org/10.2514/1.32766.

[19] Stefan, O., Constantin, S., Nicolas, M., and Jean-Francois, P., "Reduction of Landing Gear Noise Using Meshes," *16th AIAA/CEAS Aeroacoustics Conference*, Stockholm, Sweden, 2010. doi:10.2514/6.2010-3972.

[20] Okolo, P., Zhao, K., Kennedy, J., and Bennett, G., "Mesh Screen Application for Noise Reduction of Landing Gear Strut, (AIAA 2016-2845)," *22nd AIAA/CEAS Aeroacoustics Conference*, American Institute of Aeronautics and Astronautics, Lyon, France, 2016. doi:10.2514/6.2016-2845, URL http://arc.aiaa.org/doi/10.2514/6.2016-2845.

[21] Okolo, P. N., Zhao, K., Kennedy, J., and Bennett, G. J., "Numerical assessment of flow control capabilities of three dimensional woven wire mesh screens," *European Journal of Mechanics - B/Fluids*, Vol. 76, 2019, pp. 259–271. doi:10.1016/j.euromechflu.2019.03.001, URL https://linkinghub.elsevier.com/retrieve/pii/S099775461730506X.

[22] Dobrzynski, W., Schöning, B., Chow, L. C., Wood, C., Smith, M., and Seror, C., "Design and testing of low noise landing gears," *International Journal of Aeroacoustics*, Vol. 5, No. 3, 2006, pp. 233–262. doi:10.1260/1475-472X.5.3.233.

[23] John Kennedy, Elenora Neri, and Gareth J. Bennett, "The Reduction of Main Landing Gear Noise (AIAA 2016-2900)," Lyon, France, 2016. doi:10.2514/6.2016-2900, URL http://arc.aiaa.org/doi/10.2514/6.2016-2900.

[24] Rougier, T., Bouvy, Q., Casalino, D., Appelbaum, J., and Kleinclaus, C., "Design of quieter landing gears through lattice-Boltzmann CFD simulations," American Institute of Aeronautics and Astronautics, 2015. doi:10.2514/6.2015-3259, URL http://arc.aiaa.org/doi/10.2514/6.2015-3259.

[25] Gareth J. Bennett, Eleonora Neri, and John Kennedy, "Noise Characterization of a Full-Scale Nose Landing Gear," *Journal of Aircraft*, Vol. 55, No. 6, 2018, pp. 2476 – 2490. doi:10.2514/1.C034750, URL https://arc.aiaa.org/doi/10.2514/1.C034750.

[26] Chow, L., Foot, D., and Wood, C., "Aircraft noise reduction apparatus," , September 2003. The US Patent US6619587 B1.

[27] Zhao, K., Liang, Y., Yue, T., Chen, Z., and Bennett, G. J., "Characterization of the aircraft bay/landing gear coupling noise at low subsonic speeds and its suppression using leading-edge chevron spoiler," *Advances in Mechanical Engineering*, Vol. 11, No. 8, 2019, p. 168781401987143. doi:10.1177/1687814019871431, URL http://journals.sagepub.com/doi/10.1177/1687814019871431.

[28] Liang, Y., Zhao, K., Chen, Y., Zhang, L., and Bennett, G. J., "An Experimental Characterization on the Acoustic Performance of Forward/Rearward Retraction of a Nose Landing Gear," *International Journal of Aerospace Engineering*, Vol. 2019, 2019, pp. 1–11. doi:10.1155/2019/4135094, URL https://doi.org/10.1155/2019/4135094.

[29] Chow, L., Campbell, P., and Wood, C., "Landing gear noise reduction assembly," , Jan. 14 2010. URL https://www.google.com/patents/US20100006696, US Patent App. 12/458,243.

[30] Eleonora Neri, John Kennedy, Massimiliano Di Giulio, Ciaran O'Reilly, Jeremy Dahan, Marco Esposito, Massimiliano Bruno, Francesco Amoroso, Antonello Bianco, and Gareth J. Bennett, "Characterization of Low Noise Technologies Applied to a Full Scale Fuselage Mounted Nose Landing Gear," *Internoise2015: Proceedings of the Internoise 2015/ASME NCAD Meeting*, American Society of Mechanical Engineers, San Francisco, CA, USA, 2015, pp. Paper No: IN2015–350.

[31] Eleonora Neri, John Kennedy, and Gareth J. Bennett, "Bay cavity noise for full-scale nose landing gear: A comparison between experimental and numerical results," *Aerospace Science and Technology*, Vol. 72, 2018, pp. 278–291. doi:10.1016/j.ast.2017.11.016, URL http://linkinghub.elsevier.com/retrieve/pii/S1270963817314736.

[32] Zhao, K., Okolo, P., Neri, E., Chen, P., Kennedy, J., and Bennett, G. J., "Noise reduction technologies for aircraft landing gear-A bibliographic review," *Progress in Aerospace Sciences*, 2019, p. 100589. doi:10.1016/j.paerosci.2019.100589, URL https://linkinghub.elsevier.com/retrieve/pii/S0376042119300338.

[33] Wang, Y., Zhao, K., Lu, X.-Y., Song, Y.-B., and Bennett, G. J., "Bio-Inspired Aerodynamic Noise Control: A Bibliographic Review," *Applied Sciences*, Vol. 9, No. 11, 2019, p. 2224. doi:10.3390/app9112224, URL https://www.mdpi.com/2076-3417/9/11/2224.

[34] Ribeiro, A. F., Casalino, D., Fares, E., and E., N. S., "CFD/CAA Analysis of the LAGOON Landing Gear Configuration," *19th AIAA/CEAS Aeroacoustics Conference, AIAA 2013-2256*, 2013, pp. 33–43.

[35] Teruna, C., Manegar, F., Avallone, F., Ragni, D., Casalino, D., and Carolus, T., "Noise reduction mechanisms of an open-cell metal-foam trailing edge," *Journal of Fluid Mechanics*, Vol. 898, 2020, pp. 33–43.

[36] Eleonora Neri, John Kennedy, and Gareth J. Bennett, "Aeroacoustic Source Separation on a Full Scale Nose Landing Gear Featuring Combinations of Low Noise Technologies," *Internoise2015: Proceedings of the Internoise 2015/ASME NCAD Meeting*, American Society of Mechanical Engineers, San Francisco, CA, USA, 2015, pp. Paper No: NCAD2015–5912. doi:10.1115/NCAD2015-5912, URL http://proceedings.asmedigitalcollection.asme.org/proceeding.aspx?articleid=2441119.

[37] Pott-Pollenske, M., and Delfs, J., "Enhanced Capabilities of the Aeroacoustic Wind Tunnel Braunschweig," *14th AIAA/CEAS Aeroacoustics Conference (29th AIAA Aeroacoustics Conference)*, American Institute of Aeronautics and Astronautics, Vancouver, British Columbia, Canada, 2008. doi:10.2514/6.2008-2910, URL https://arc.aiaa.org/doi/10.2514/6.2008-2910.